arXiv:cond-mat/0504569v2 [cond-mat.mes-hall] 3 Aug 2005

Polarization and Aharonov-Bohm oscillations in quantum-ring magnetoexcitons

Luis G. G. V. Dias da Silva,[1,*] Sergio E. Ulloa,[1] and Tigran V. Shahbazyan[2]
[1]*Department of Physics and Astronomy, Nanoscale and Quantum Phenomena Institute, Ohio University, Athens, Ohio 45701-2979*
[2] *Department of Physics and Computational Center for Molecular Structure and Interactions, Jackson State University, Jackson, MS 39217*

(Dated: February 2, 2008)

We study interaction and radial polarization effects on the the absorption spectrum of neutral bound magnetoexcitons confined in quantum-ring structures. We show that the size and orientation of the exciton's dipole moment, as well as the interaction screening, play important roles in the Aharonov-Bohm oscillations. In particular, the excitonic absorption peaks display A-B oscillations both in position and amplitude for weak electron-hole interaction and large radial polarization. The presence of impurity scattering induces anticrossings in the exciton spectrum, leading to a modulation in the absorption strength. These properties could be used in experimental investigations of the effect in semiconductor quantum-ring structures.

PACS numbers: 73.21.La, 21.60.Jz 65.80.+n

I. INTRODUCTION

The manifestation of the optical Aharonov-Bohm[1] (AB) effect in neutral and charged excitons in semiconductor quantum rings has received considerable attention in recent years from both theoretical[2,3,4,5,6,7,8,9,10,11,12,13] and experimental[14,15] groups. In contrast to the cumulative-phase ABE in electronic systems,[16,17] the optical ABE originates from the difference between the phases acquired by the electron and hole wave functions as the magnetic flux threads the ring. Such phase differences can be probed by standard photoluminescence (PL) experiments since the change in phase is accompanied by a change in the exciton's total angular momentum, making the optical emission field-dependent through dipole selection rules.[3,4,5,6,7]

It has been shown[5] that the AB effect is weak when both the electron and the hole forming the neutral exciton are confined within the same ring geometry. However, an enhancement of this effect is expected when the exciton is *radially polarized*, either by the application of an external electric field[8] or due to a radial asymmetry in the effective confinement for electrons and holes.[9,10,11,13] In the latter case, differences in the valence and conduction band profiles lead to different *effective* ring radii for holes and electrons, and therefore distinct magnetic flux, giving rise to a field-dependent *phase difference* between the electron and hole wave functions. The resulting excitonic AB effect stems from the effective magnetic phase acquired by the wave function of an electron-hole pair as it goes around the ring.

For a non-interacting electron-hole pair with different ring radii ($R_e \neq R_h$), the optical AB effect is expected to manifest itself as a modulation in the PL energy and intensity.[9] Experimental verification of this effect has been recently reported[15] in PL measurements of radially polarized excitons in a type-II quantum dot structure.[18] To date, however, no comprehensive study of optical properties in quantum-ring magnetoexcitons that fully includes the electron-hole interaction in a non-perturbative way, along with the ring-confinement and exciton polarization, has been reported.

In this paper, we show that the optical absorption in semiconductor quantum rings is governed by the interplay between Coulomb interactions and the excitonic radial polarization. The model for the polarized quantum-ring magnetoexcitons is presented in Sec. II and our main results are shown in Sec. III. Ground-state AB oscillations are prominent when interactions are weak (due to, e.g., strong screening by a metallic gate), and the oscillatory pattern changes when the electric dipole vector is reversed, as shown in Sec. III A. In the fully interacting (weak screening) regime (Sec. III B), the oscillations are suppressed in the lowest optically active state due to the "Coulomb locking" of the electron and the hole. Moreover, as the magnetic field increases, the ground-state changes its angular momentum from 0 to 1, becoming optically inactive, and corroborating an earlier qualitative analysis of the strongly interacting limit.[9] The optically active excited states are shown to display a rich structure of AB oscillations and field-dependent absorption modulations. Most importantly, we show that the gap between the ground and the excited states can be tuned by changing the exciton's electric dipole moment, allowing for an experimental characterization of the excited states of quantum-ring structures.

Furthermore, in Sec. III C we analyze how the scattering due to impurities along the ring affects the optical absorption. The impurity-induced coupling between exciton states leads to a modulation in the absorption as a function of magnetic field, present even for very weak scattering potential strengths.

II. MODEL

Our model describes the optical absorption by neutral polarized excitons in the presence of a perpendicular magnetic field. The electron and hole forming the exciton are restricted to one-dimensional ($1D$) concentric rings with radii R_e and R_h, respectively. In this approximation, the exciton Hamiltonian in the presence of external fields reads:

$$H = \sum_l \Big[[\varepsilon_e (l+\phi_e)^2 + E_g] a_l^\dagger a_l + \varepsilon_h (l-\phi_h)^2 b_l^\dagger b_l \Big] \\ - \sum_{ll'q} v_q a_{l+q}^\dagger b_{l'-q}^\dagger b_{l'} a_l - \mu E(t) \sum_l (a_l^\dagger b_{-l}^\dagger + h.c.), \quad (1)$$

where a_l (b_l) annihilates an electron (hole) with integer-valued angular momentum l, $\varepsilon_i = \hbar^2/(2m_i R_i^2)$ ($i = e, h$) is the size-quantization energy for each ring, $\phi_i = \pi R_i^2 B/\phi_0$ is the magnetic flux through the ith ring in units of $\phi_0 = he/c$, B is the magnetic field, $E(t) = E_0 \cos \omega t$ is the electric field of incident light, μ is the interband matrix element, and E_g is the optical bandgap. The electron-hole potential matrix elements, calculated from the wave functions in the rings, are given in terms of toroidal functions[19]

$$v_q = \frac{e^2}{\pi \epsilon_r \bar{R}} Q_{|q|-1/2} \left[1 + \frac{d^2}{2\bar{R}^2} \right], \quad (2)$$

where ϵ_r is the dielectric constant of the environment, $d = |R_h - R_e|$ is the inter-ring separation, $\bar{R} = \sqrt{R_e R_h}$ is the geometrical average radius, and $Q_\mu(x)$ is the Legendre function. When $\bar{R} \gg d$, the potential simplifies to a more amenable form

$$v_q = \frac{e^2}{\pi \epsilon_r \bar{R}} K_0 \left[\frac{(q+1/2)d}{\bar{R}} \right], \quad (3)$$

where $K_0(x)$ is the modified Bessel function.

In the absence of impurity scattering (which will be discussed in Sec. III C), light absorption (emission) is determined by the optical polarization due to excitation of an electron-hole pair with zero total angular momentum ($L \equiv l_e + l_h = 0$), namely,[20]

$$P(t) = 2\mu \sum_l p_l(t) = 2\mu \sum_l \langle b_{-l} a_l \rangle. \quad (4)$$

The equation for the microscopic polarization components $p_l(t)$ can be obtained from the Heisenberg equation of motion for the operator $b_{-l} a_l$,[20]

$$\frac{i\partial p_l}{\partial t} - \Big[\varepsilon_e (l+\phi_e)^2 + \varepsilon_h (l+\phi_h)^2 + E_g \Big] p_l \\ + \sum_{l'} v_{l-l'} p_{l'} = -\mu E(t). \quad (5)$$

In the rotating wave approximation, the frequency-dependent polarization $p_l(\omega)$ is determined from

$$\Big[\Omega + i\gamma - \varepsilon_e (l+\phi_e)^2 - \varepsilon_h (l+\phi_h)^2 \Big] p_l \\ + \sum_{l'} v_{l-l'} p_{l'} = -\mu E_0/2, \quad (6)$$

where $\Omega = \omega - E_g$ is the detuning of the incident light from the band edge, and γ is the homogeneous broadening. The solution of the system of coupled equations given by (6) determines the absorption coefficient,[20]

$$\alpha(\omega, B) = \frac{4\pi\omega}{n\epsilon_r E_0} \mathrm{Im} P(\omega, B) = \frac{8\pi\mu\omega}{n\epsilon_r E_0} \mathrm{Im} \sum_l p_l(\omega, B), \quad (7)$$

which is a function of the incident light frequency ω, and of the magnetic field B. Note that resonances of $\alpha(\omega, B)$ occur at frequency values corresponding to exciton eigenstates which are directly coupled to radiation (dipole active), i.e. states with zero total angular momentum ($l_e = -l_h$).

The truncation implemented in the calculation is set by the maximum angular momentum value $-l_{\max} \leq l \leq l_{\max}$, so that there are $2l_{\max}+1$ coupled equations. In the following, we use $l_{\max} \sim 30$, which gives reliable results for all the optically active states of interest.

III. ABSORPTION RESULTS

We calculate the absorption coefficient $\alpha(\omega, B)$ for different model parameters. In the following, we have set $\gamma = 0.05$meV and $E_g = 1.5$eV, which are in the range of actual experimental values. For concreteness, we take the electron effective mass to be $m_e = 0.0073 m_0$ (InP value) and set $m_h = 3.5 m_e$. The E_0 and μ values determine the amplitude of the absorption coefficient, so that α is reported in those units.

In terms of the effectiveness of the attractive Coulomb potential screening, we consider two distinct regimes: (i) a "weakly-bound" regime, where the effective screening caused by metal contacts and nearby image charges is much larger than the bulk dielectric screening of the material and (ii) a "fully interacting" regime, where the usual bulk dielectric screening is considered. The two regimes are characterized by the strength of the Coulomb interaction, as reduced by the factor ϵ_r. For simplicity, we characterize the weakly and fully interacting regimes by setting the dielectric constant to $\epsilon_r = 100$, and $\epsilon_r = 10$, respectively.

A. Weakly-bound regime

Results for the ground-state absorption in the weakly-bound case are shown in Fig. 1. The absorption peak position displays an overall parabolic diamagnetic blueshift, so that the exciton binding energy ($-\Omega$, at the peak) decreases with magnetic field, as expected. Most importantly, an oscillation in both peak position *and* peak height is superimposed on the parabolic shift.

These ground-state oscillations in energy and absorption strength for the weakly-bound exciton constitute the signature of the optical Aharonov-Bohm effect and have been studied previously.[9,10,11,13] We should emphasize

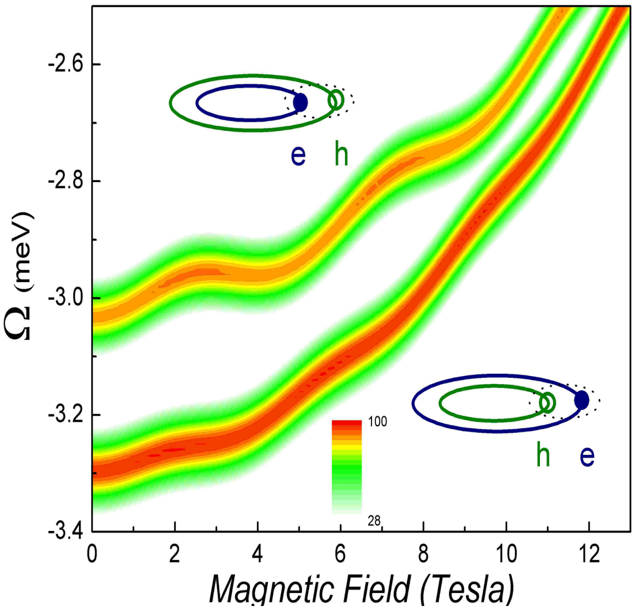

FIG. 1: (color online) Absorption of the lowest optically active state, shown as color maps, for the weakly bound regime ($\epsilon_r = 100$), with $R_e = 16nm$ and $R_h = 20nm$ (top map) and $R_e = 20nm$ and $R_h = 16nm$ (bottom map). Notice energy and absorption strength oscillations with field. Scale is normalized to the highest absorption value (= 100).

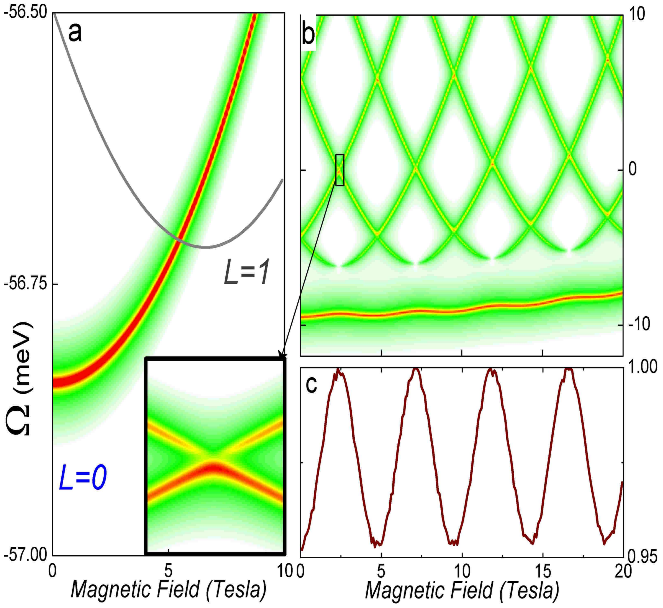

FIG. 2: (color online) Optical absorption for the fully interacting regime ($\epsilon_r = 10$) with $R_e = 16nm$ and $R_h = 20nm$. Left panel: The absorption peak follows the lowest $L = 0$ state, which is the ground state for low field and show no ABE oscillations. The "dark" low-lying $L = 1$ state (solid line, calculated from numerical diagonalization) becomes the ground state for $B \approx 5.5T$. Right panels: Absorption from the optically active excited states. Oscillations in both peak position (top) and peak height (bottom) are observed as function of magnetic field. Fig. 2c depicts the maximum value of the absorption peak corresponding to the first excited state. Absorption variations are also present on excited state anticrossings (Inset on left panel).

that these prior analysis are based on a non-interacting picture, with the oscillations arising from the different dispersions for electrons and holes. We show that such ground-state oscillations remain only for very weak interaction strengths. The curvature and period of the oscillations depend on the single-particle dispersions and on whether the electron or the hole is in the inner ring, as shown in Fig. 1. Notice that the oscillations in energy and the contrast in the peak height modulation are more pronounced when the electron, the lighter particle, is in the inner ring. In other words, the ground-state AB oscillations and the exciton binding energy are affected by a π rotation in the electric radial dipole direction.

This behavior can be understood by noting that, in the case of a *non-polarized* exciton in a ring of radius R, the AB oscillations in the lowest $L = l_e + l_h = 0$ state (which, for $R_e = R_h = R$, is the ground state) are suppressed by a factor $\exp(-|v_0|/E_0)$, where $|v_0|$ is the interaction matrix element strength and $E_0 = \hbar^2/2\mu R^2$, with $\mu = m_e m_h/(m_e + m_h)$ the reduced mass of the electron-hole pair.[5,7] This factor represents the probability of exciton dissociation due to the finite ring size. For a polarized exciton ($R_e \neq R_h$), a similar analysis shows that this factor becomes approximately $\exp(-|v_0|/E_p)$, with $E_p = \hbar^2/2I_{\text{red}}$, where $I_{\text{red}} = I_e I_h/(I_e + I_h)$ is the reduced moment of inertia of the electron-hole pair ($I_{e(h)} \equiv m_{e(h)} R^2_{e(h)}$). Since $m_e < m_h$, one expects a lower attenuation of the effect if $R_e < R_h$. In a similar fashion, the zero-field exciton binding energy, which scales with E_p, will also be lower for $R_e < R_h$. This corroborates the results shown in Fig. 1.

B. Fully interacting regime

The picture is qualitatively different in the fully interacting regime (Fig. 2). As expected, the exciton binding energy is substantially larger than in the weakly bound case. At the same time, the absorption peak, corresponding to the lowest optically active ($L = 0$) state, shows an uniform diamagnetic blueshift, with no oscillatory behavior. The absence of the Aharonov-Bohm oscillations is caused by the *locking* of electron and hole due to the Coulomb attraction. Note that, in 1D, the effective strength of the Coulomb interaction is larger than in higher dimensions and, correspondingly, so is the exciton binding energy. In the fully interacting regime, the exciton wave-function with a given L has no magnetic flux dependence and the AB effect manifests itself as a periodic change of the ground state angular momentum.[9] In particular, the $L = 0$ state becomes higher in energy than the first $L = 1$ state at a certain magnetic field ($B \approx 5.5$

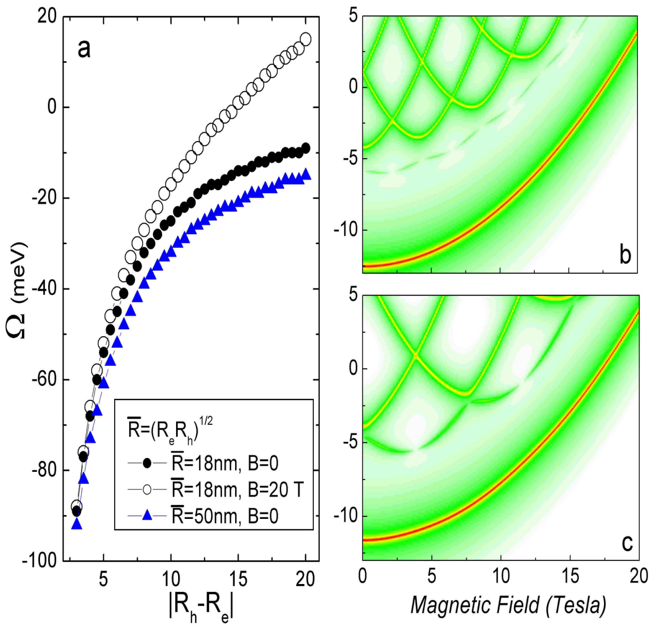

FIG. 3: (color online) Left: Ground-state energy as a function of the exciton dipole moment in the fully interacting regime. Right: Optical absorption for $d = |R_e - R_h| = 19$nm: $R_e = 16nm$ and $R_h = 35nm$ ($\bar{R} = 23.67$nm, top) and $R_e = 12nm$ and $R_h = 27nm$ ($\bar{R} = 18$nm, bottom). The binding energy remains essentially constant but the excited state oscillation period decreases as $\bar{R}$ increases.

T for the parameters of Fig. 2). As the magnetic field is further increased, this $L = 1$ ground state is replaced by a $L = 2$ state and so on. Since only the $L = 0$ state is optically active, observation of AB oscillations in the lowest absorption peak is inhibited in the strongly interacting regime. By contrast, in the weakly-bound regime, the $L = 0$ state itself is modulated, resulting in optically observable AB oscillations.

Our calculations also reveal an intricate structure of the (optically active) excited states, as shown in the right-hand panels of Fig. 2. The first excited state is still bound (binding of ≈ 9 meV) and has a clear oscillatory character similar to that in the weakly-bound ground state, due to lower Coulomb barrier, with oscillations in both energy (Fig. 2b) and strength (Fig. 2c, which shows the maximum height of the absorption peak as a function of field). The higher states present an even more complicated structure, with anti-crossings at $\phi_e/\phi_0 \approx n/2$ (where n is an integer). A closer look (inset) shows that the absorption strength at the anti-crossing is non-symmetric: it is enhanced for one of the states and suppressed for the other.

A rather remarkable feature is a strong sensitivity of the absorption spectrum to the variations of the exciton polarization, as shown in Fig. 3. In the fully interacting regime, the exciton binding energy is reduced as the exciton dipole moment $D = e|R_e - R_h|$ is increased (Fig. 3a). This is expected, since the interaction potential (Eq. (2)) is modified as both the average radius $\bar{R}$ and $d = |R_e - R_h|$ change. Another important consequence is that the gap ΔE between lowest and the first excited optically active states can be tuned by changing D. For a large D, even though the ground state does not show oscillations (Figs. 3b-c), ΔE is strongly reduced (from $\Delta E \sim 50$ meV at $d = 4$nm to $\Delta E \sim 8$ meV at $d = 19$nm). We also show that, albeit the binding energy depends only weakly on $\bar{R}$ (Fig. 3a), the excited states's oscillation period decreases as $\bar{R}$ increases (Figs. 3b-c).

C. Impurity effects

We extend the analysis of the previous sections by studying the effect of an impurity scattering center in the optical absorption coefficient. We consider the scattering of electrons and holes due to a localized impurity potential at an angular position $\theta_{\rm imp}$ in the ring. Such scattering can be accounted for by including a term in the exciton Hamiltonian (1) of the form:

$$H_{\rm imp} = \sum_{ll'} U_e(l,l') a_l^\dagger a_{l'} + U_h(l,l') b_l^\dagger b_{l'} \; , \qquad (8)$$

where the impurity potential $U_{e(h)}(l,l') \equiv \exp i(l - l')\theta_{\rm imp}^{e(h)}$ scatters electrons (holes), changing the angular momentum from l to l', thus coupling different single-particle $|l\rangle$ states. The rotational symmetry of the system is thus broken and the exciton angular momentum $L = l_e + l_h$ no longer commutes with the Hamiltonian. For simplicity, we consider a single impurity located at $\theta_{\rm imp}^{e(h)} = 0$ so $U_{e(h)}(l,l')$ is a constant, with no dependance in l, l' (a different $\theta_{\rm imp}^{e(h)}$ only adds a phase to $U_{e(h)}$). In the following, the values of U_e and U_h are given in units of the single-particle energy scales $\varepsilon_i = \hbar^2/(2m_i R_i^2)$ ($i = e, h$).

Due to the rotational symmetry breaking, excitonic states with distinct L are now connected by $H_{\rm imp}$ and the optical properties will no longer be determined solely from the "bright" ($L = 0$) states but will have contributions from the "dark" excitonic states as well.[13] In order to calculate the optical absorption, we generalize the approach described in Sec. II, by using the equation of motion for the operator $b_{l'} a_l$. This gives a set of coupled equations for the components $P_{ll'} \equiv \langle b_{l'} a_l \rangle$ and the frequency-dependent components $P_{ll'}(\omega)$ are determined from a generalized form of eqs. (6), namely:

$$\begin{aligned} &\Big[\Omega + i\gamma - \varepsilon_e(l+\phi_e)^2 - \varepsilon_h(l'-\phi_h)^2 + E_g\Big] P_{ll'} \\ &\quad - \left(\sum_{l''} U_e(l,l'') P_{l''l'} + U_h(l',l'') P_{ll''}\right) \\ &\quad\quad + \sum_q v_q P_{(l-q)(l'+q)} = -\delta_{l(-l')} \mu E_0/2, \qquad (9) \end{aligned}$$

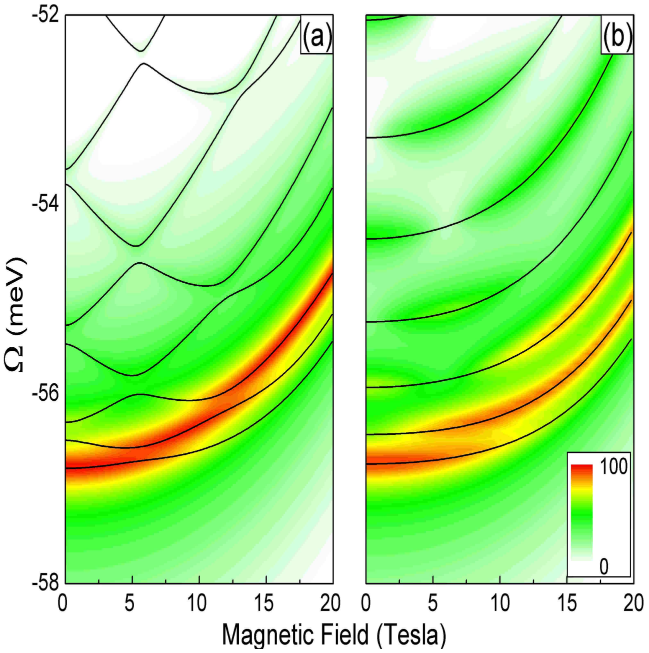

FIG. 4: (color online) Absorption coefficient for the impurity case, shown as a color map, for the fully interacting regime ($\epsilon_r = 10$) with $R_e = 16nm$ and $R_h = 20nm$ and increasing impurity potential strength. The lines correspond to the energy eigenvalues calculated by direct diagonalization. (a) $U_{e(h)} = 0.05\varepsilon_{e(h)}$ and (b) $2\varepsilon_{e(h)}$ respectively. Notice anticrossings in the energy levels, optical emission from "dark" states due to impurity scattering, and energy and absorption strength oscillations with field. Scale is normalized to the highest absorption value (= 100).

and the absorption coefficient will be given by:

$$\alpha(\omega, B) = \frac{8\pi\mu\omega}{n\epsilon_r E_0} \mathrm{Im} \sum_l P_{l(-l)}(\omega, B) \; . \qquad (10)$$

By setting $U_e = U_h = 0$ (no impurity scattering) and $l' = -l$ in eqs. (9-10), one recovers eqs. (6-7) and the structure of absorption peaks following the $L = 0$ eigenstates, shown in Fig. 2. Such structure is strongly modified when impurities are present, i.e., for non-zero values of $U_{e(h)}$.

Fig. 4 shows impurity effects in the absorption spectrum for the same ring parameters as in Fig. 2. For low values of the impurity potential, anticrossings in the spectrum appear due to the coupling between states with different L (Fig. 4a). Most importantly, this coupling also results in the appearance of *new* absorption peaks, at energies corresponding to otherwise dark states. In particular, the main absorption peak splits at the magnetic field values where the ground-state anticrossings occur, generating an impurity-induced *modulation* of the absorption strength as a function of magnetic field.

This splitting is further enhanced for larger values of $U_{e(h)}$ (Fig. 4b). In this case, the dependence of the energy levels with magnetic field is essentially parabolic due to the strong localization of the exciton wavefunction in the ring by the impurity potential.[13] In addition to the large splittings in the main absorption peak, a series of secondary peaks appear and disappear as a function of magnetic field, their positions following the ground and excited states' energies.

IV. CONCLUDING REMARKS

To summarize, we have studied polarization effects in the optical absorption of neutral excitons in semiconductor quantum rings. The ground state displays AB oscillations in the weakly bound regime and both the oscillation period and the binding energy are affected by the exciton's dipole moment in the radial direction. In the strongly interacting regime, oscillations in the absorption are suppressed due to the Coulomb locking of the electron and hole in the lowest optically active state, whereas the AB effect manifests itself in a "bright → dark" transition in the ground state as the magnetic field increases. Nevertheless, AB oscillations in the absorption should be observable for the excited states, whose excitation energy can be tuned by the varying the exciton dipole moment, even in the fully interacting regime. Furthermore, a mixing of bright and dark exciton states is expected when scattering from charge impurities is included in the analysis, leading to anticrossings in the absorption spectrum.

We propose three ways in which experimental verification of our predictions could be attained in PL emission setups in samples with low impurity concentration: (i) ABE oscillations in the optically active ground-state could be measured if the attractive Coulomb interaction between the electron and hole is sufficiently screened, which can be achieved by placing a doped substrate layer or nearby metal contacts to the sample. (ii) A strong radial polarization of the exciton would reduce the excitation gap necessary to probe into the ABE-sensitive excited states. If the gap is below the optical phonon threshold, the main relaxation process becomes the emission of acoustic phonons. This may give rise to high-energy (excited state) peaks in the PL signal, allowing one to probe the AB oscillations. (iii) In the fully-interacting and low-polarization regime, the excitonic ground state becomes "dark" at a certain magnetic field. At this value of the magnetic field, one expects an abrupt reduction in the exciton's relaxation lifetime, which could be probed with time-resolved PL spectroscopy.

As some degree of impurity scattering is expected in actual samples, this picture can be qualitatively modified. The presence of localized impurities at the ring's edge allows coupling between bright and dark exciton states, resulting in a modulation in the absorption strength as a function of magnetic field and the appearance of secondary peaks at energy values corresponding to otherwise dark exciton states.

Acknowledgments

We thank A. Govorov for valuable conversations and suggestions. This work was partially supported by NSF-IMC and NSF-NIRT grants. T.V.S. acknowledges support from NSF grants DMR-0305557 and NUE-0407108, and ARL grant DAAD19-01-2-0014.

---

[*] Electronic address: gregorio@phy.ohiou.edu

[1] Y. Aharonov and D. Bohm, Phys. Rev., **115**, 485 (1959).

[2] P. Pereyra, S. E. Ulloa, Phys. Rev. B **61**, 2128 (2000).

[3] A. O. Govorov, A. V. Chaplik, JETP Lett. **66**, 454 (1997).

[4] A. V. Chaplik, JETP Lett. **62**, 900 (1995).

[5] R. A. Römer, M. E. Raikh, Phys. Rev. B **62**, 7045 (2000).

[6] J. Song, S. E. Ulloa, Phys. Rev. B **63**, 125302 (2001).

[7] H. Hu, J.-L. Zhu, D.-J. Li and J.-J Xiong, Phys. Rev. B **63**, 195307(2001).

[8] A. V. Maslov, D. S. Citrin, Phys. Rev. B **67**, 121304(R) (2003).

[9] A. O. Govorov, S. E. Ulloa, K. Karrai, R. J. Warburton, Phys. Rev. B **66**, 081309(R) (2002)

[10] S. E. Ulloa, A. O. Govorov, A. B. Kalameitsev, R. J. Warburton, K. Karrai, Physica E **12**, 790 (2002).

[11] A. O. Govorov, A. B. Kalameitsev, R. J. Warburton, K. Karrai, S. E. Ulloa, Physica E **13**, 297 (2002).

[12] J. I. Climente, J. Planelles, W. Jaskolski, Phys. Rev. B **68**, 075307 (2003).

[13] L. G. G. V. Dias da Silva, S. E. Ulloa, A. O. Govorov, Phys. Rev. B **70**, 155318 (2004).

[14] M. Bayer, M. Korkusinski, P. Hawrylak, T. Gutbrod, M. Michel, and A. Forchel, Phys. Rev. Lett. **90**, 186801 (2003).

[15] E. Ribeiro, A.O. Govorov, W. Carvalho, G. Medeiros-Ribeiro, Phys. Rev. Lett. **92**, 126402 (2004).

[16] A. Lorke, R. J. Luyken, A. O. Govorov, J. P. Kotthaus, J. M. Garcia, P. M. Petroff, Phys. Rev. Lett. **84**, 2223 (2000).

[17] P. M. Petroff, A. Lorke, A. Imamoglu, Phys. Today **54** (5), 46 (2001).

[18] A. B. Kalameitsev, V. M. Kovalev, A. O. Govorov, JETP Lett. **68**, 669 (1998).

[19] T. V. Shahbazyan, S. E. Ulloa, Phys. Rev. B **55**, 13702 (1997).

[20] H. Haug and S. W. Koch, *Quantum Theory of Optical and Electronic Properties of Semiconductors* (World Scientific, 1993).